## Title

Early Assessment of Molecular Progression and Response by Whole-genome Circulating Tumor DNA in Advanced Solid Tumors.



## Journal

Molecular Cancer Therapeutics, 19(7)

## Authors

Lentz, Robert
Peterman, Neil
Robertson, Alex
et al.

## Publication Date

2020-07-01

## DOI

10.1158/1535-7163.MCT-19-1060

Peer reviewed

Published in final edited form as:

*Mol Cancer Ther*. 2020 July ; 19(7): 1486–1496. doi:10.1158/1535-7163.MCT-19-1060.

# Early Assessment of Molecular Progression and Response by Whole-genome Circulating Tumor DNA in Advanced Solid Tumors

**Andrew A. Davis**[1,2], **Wade T. Iams**[3], **David Chan**[4], **Michael S. Oh**[1], **Robert W. Lentz**[1], **Neil Peterman**[5], **Alex Robertson**[5], **Abhik Shah**[5], **Rohith Srivas**[5], **Timothy J. Wilson**[5], **Nicole J. Lambert**[5], **Peter S. George**[5], **Becky Wong**[5], **Haleigh W. Wood**[5], **Jason C. Close**[5], **Ayse Tezcan**[5], **Ken Nesmith**[5], **Haluk Tezcan**[5], **Young Kwang Chae**[1,2]

[1]Feinberg School of Medicine, Northwestern University, Chicago, Illinois

[2]Robert H. Lurie Comprehensive Cancer Center of Northwestern University, Chicago, Illinois

[3]Vanderbilt University Medical Center, Nashville, Tennessee

[4]Cancer Care Associates TMPN, Redondo Beach, California

[5]Lexent Bio, Inc., San Francisco and San Diego, California

## Abstract

Treatment response assessment for patients with advanced solid tumors is complex and existing methods require greater precision. Current guidelines rely on imaging, which has known limitations, including the time required to show a deterministic change in target lesions. Serial changes in whole-genome (WG) circulating tumor DNA (ctDNA) were used to assess response or resistance to treatment early in the treatment course. Ninety-six patients with advanced cancer were prospectively enrolled (91 analyzed and 5 excluded), and blood was collected before and after initiation of a new, systemic treatment. Plasma cell–free DNA libraries were prepared for either WG or WG bisulfite sequencing. Longitudinal changes in the fraction of ctDNA were quantified to retrospectively identify molecular progression (MP) or major molecular response (MMR). Study endpoints were concordance with first follow-up imaging (FFUI) and stratification

**Corresponding Authors:** Young Kwang Chae, Northwestern University Feinberg School of Medicine, 645 N. Michigan Avenue, Suite 1006, Chicago, IL 60611. Phone: 312-926-4248; Fax: 312-695-0370; young.chae@northwestern.edu; and Haluk Tezcan, 10355 Science Center Dr, #150; San Diego, CA 92121. htezcan@lexentbio.com.

Authors' Contributions

**Conception and design:** A.A. Davis, W.T. Iams, N. Peterman, R. Srivas, T.J. Wilson, A. Tezcan, K. Nesmith, H. Tezcan, Y.K. Chae

**Development of methodology:** A.A. Davis, W.T. Iams, R.W. Lentz, N. Peterman, R. Srivas, T.J. Wilson, N.J. Lambert, B. Wong, H.W. Wood, A. Tezcan, H. Tezcan, Y.K. Chae

**Acquisition of data (provided animals, acquired and managed patients, provided facilities, etc.):** A.A. Davis, W.T. Iams, D. Chan, M.S. Oh, R.W. Lentz, R. Srivas, N.J. Lambert, B. Wong, H.W. Wood, J.C. Close, A. Tezcan, H. Tezcan, Y.K. Chae

**Analysis and interpretation of data (e.g., statistical analysis, biostatistics, computational analysis):** A.A. Davis, N. Peterman, A. Robertson, A. Shah, R. Srivas, A. Tezcan, H. Tezcan, Y.K. Chae

**Writing, review, and/or revision of the manuscript:** A.A. Davis, W.T. Iams, D. Chan, N. Peterman, A. Robertson, R. Srivas, N.J. Lambert, P.S. George, A. Tezcan, K. Nesmith, H. Tezcan, Y.K. Chae

**Administrative, technical, or material support (i.e., reporting or organizing data, constructing databases):** A.A. Davis, M.S. Oh, N. Peterman, R. Srivas, P.S. George, A. Tezcan, H. Tezcan

**Study supervision:** D. Chan, A. Tezcan, H. Tezcan, Y.K. Chae

**Other (performed wet-lab work):** P.S. George

**Other (preparation and sequencing of NGS libraries from patient plasma):** J.C. Close

**Note:** Supplementary data for this article are available at Molecular Cancer Therapeutics Online (http://mct.aacrjournals.org/).

of progression-free survival (PFS) and overall survival (OS). Patients with MP ($n$ = 13) had significantly shorter PFS (median 62 days vs. 310 days) and OS (255 days vs. not reached). Sensitivity for MP to identify clinical progression was 54% and specificity was 100%. MP calls were from samples taken a median of 28 days into treatment and 39 days before FFUI. Patients with MMR ($n$ = 27) had significantly longer PFS and OS compared with those with neither call ($n$ = 51). These results demonstrated that ctDNA changes early after treatment initiation inform response to treatment and correlate with long-term clinical outcomes. Once validated, molecular response assessment can enable early treatment change minimizing side effects and costs associated with additional cycles of ineffective treatment.

## Introduction

The current standard of care for clinical evaluation of treatment response for advanced solid tumors is based on physical exams, patient reported symptoms, and periodic radiographic tumor assessments to determine whether the patient is responding or progressing while on treatment. However, there are limitations to these approaches as subtle changes in disease are often asymptomatic, and considerable costs, uncertainty, and anxiety can be associated with frequent imaging. In clinical trials, imaging response criteria are standardized to guide evaluation by comparing a baseline scan before treatment initiation with periodic follow-up imaging with prespecified criteria for response (1, 2). These criteria can be limited by the reliability of measurements over time, difficult to measure sites of disease (e.g., bone or pleural effusions), and challenges distinguishing pseudoprogression from true progression (3–5). In addition, interoperator variability in comparing serial scans remains a limitation in response assessment (6). Therefore, novel methods for monitoring response to treatment are needed given the emergence of new treatment modalities with ongoing questions regarding how best to manage treatment, minimize toxicity, and control costs.

Liquid biopsy assays in patients with cancer may analyze circulating cell-free DNA (cfDNA), circulating tumor cells, RNA, exosomes, or proteins (7, 8). Circulating tumor DNA (ctDNA) likely originates from cancer cells undergoing apoptosis, necrosis, or potential active mechanisms involving nucleic acid secretion to facilitate metastasis and gene expression at distant sites (9). The amount of ctDNA correlates with more advanced stages of disease and is also affected by tumor type, origin, location of metastasis, and treatment (10, 11). There are several distinguishing features between ctDNA and nontumor cfDNA. Specifically, as compared with cfDNA, ctDNA contains tumor-specific somatic point mutations, structural variations, shorter fragment lengths, biased fragment start and end positions, and changes in epigenetic patterns (12–19). Copy-number aberrations (CNA), which consist of either deletions or duplications of portions of the genome, are a common form of structural variation that are observed in patients with advanced disease at various sites across the genome (20). Prior studies have demonstrated that CNAs can be detected in cfDNA from patients by low-pass next-generation sequencing (NGS) with CNAs detected at a higher rate in patients with advanced disease (21, 22). To date, changes in CNAs over time in patients with advanced cancer remain understudied. Global hypomethylation is a hallmark of tumor genomes (19, 23), and an increase in global methylation levels in cfDNA might be associated with response as it would indicate a decreased proportion of ctDNA. Importantly,

the epigenetic patterns observed in tumors, including overall global hypomethylation can be detected in ctDNA and could therefore have potential for tracking patients over time (24, 25).

Recently, there has been significant interest in evaluating the potential clinical utility of ctDNA in advanced solid tumors. In the adjuvant setting, residual ctDNA after surgery (e.g., minimal residual disease) has been associated with disease recurrence across multiple tumor types (11, 26–29). In advanced disease, the most well-validated clinical use is to identify driver mutations with known drug targets (30–33). In addition, resistance mutations have been identified in the blood with the goal of guiding clinical management (34). While prior studies have evaluated the potential role of tracking ctDNA for tumor response assessment by tracking mutant allele frequencies or particular mutations, the clinical utility for routine assessment has not yet been established (11, 12, 35–40).

Here, in a prospectively enrolled, advanced stage, pan-cancer cohort, we performed whole-genome analysis of ctDNA as a response assessment earlier in the treatment course compared with routine clinical and radiographic assessment of disease. In contrast to analyzing particular genes, our approach utilized CNAs and fragmentation patterns across the genome, a technique with broad potential clinical applications across multiple tumor types. We hypothesized that early changes in cancer-associated signals in the blood would be predictive of response status at the time of first follow-up imaging (FFUI) and that the magnitude of the dynamic change in signal would provide longer term prognostic information across a variety of solid tumor types and treatments.

## Materials and Methods

### Study participants

The study sample here represented a subset of a currently accruing longitudinal observational study (NCT02288754). From May 2017 to December 2018, participants (age > 18 years) were prospectively enrolled from five oncology centers in the United States (TMPN - Cancer Care, Redondo Beach, CA; Scripps - California Cancer Associates, San Diego, CA; Sharp Memorial Hospital, San Diego, CA; Summit Cancer Centers, Post Falls, ID; and Robert H. Lurie Comprehensive Cancer Center of Northwestern University, Chicago, IL) and followed through September 2019 (Table 1). Eighty percent of the participants in this analysis came from one center (Supplementary Table S1). Eligibility criteria were:

- **i.** Diagnosis of a nonhematologic and surgically unresectable advanced tumor (stage III or IV) at registration.
- **ii.** Commencement of a new systemic treatment regimen of the physician’s choice.
- **iii.** Presence of either measurable or evaluable disease by imaging before treatment initiation.

To be included in this cohort, the participants needed to have venous blood samples from at least two time points: at baseline (T0, before treatment initiation) and another one before cycle 2 (T1) and/or cycle 3 (T2; Fig. 1A). Sample collection was performed to align with

standard clinical visits for patient convenience. The timing in this study was in-line with prior work optimizing the collection timing of liquid biopsy samples for use as a surrogate for progression-free survival (PFS; ref. 39). The study reported here was conducted in accordance with the Declaration of Helsinki and approved by Northwestern University (Chicago, IL), Sharp Memorial Hospital (San Diego, CA), and Western Institutional Review Boards. Written informed consent was obtained from each patient prior to participation in the study.

## Evaluation of response status

Participants were radiologically assessed at baseline and again at FFUI as determined per standard-of-care routine clinical assessment. The primary endpoint of the study was evidence of radiographic progression as determined by RECIST version 1.1 (1) or clinical response evaluation. Measurable disease changes by imaging were interpreted by an independent radiologist, who was blinded to the assessment of molecular response. Radiographic assessments were categorized as progressive disease (PD) or non-PD (nonPD), which included partial response (PR), stable disease (SD), and complete response.

Overall survival (OS) was defined as the time from the start of treatment to death due to any cause. PFS was defined as the time from the start of treatment to first documentation of PD, or death due to any cause, whichever occurred first.

## Sample preparation

At each timepoint, 10 mL of whole blood was collected in Streck Cell-Free DNA BCT. Plasma was separated via centrifugation at 1,600 × *g* for 15 minutes followed by 2,500 × *g* for 10 minutes within 7 days from the time of collection. cfDNA was extracted from plasma using the Qiagen QIAmp MinElute ccfDNA Kit and stored at −20°C until library preparation. For each patient, libraries were prepared using the KAPA HyperPrep Library Prep Kit for whole-genome sequencing (WGS; $n = 53$ patients) or the Nugen Ovation Ultralow Methyl-Seq Whole-Genome Bisulfite Sequencing Kit (WGBS; $n = 38$ patients). Average input cfDNA into the library preparation was 20 ng. Libraries were sequenced on the Illumina HiSeq X to an average depth of 20 (range 6–29).

## Bioinformatics methods

Reads were aligned to the human genome (GRCh37) with a custom bioinformatics pipeline based on BWA (41), sambamba (42), and samtools (43). WGBS libraries were processed with an adapted pipeline to align sequencing data to a bisulfite-converted human genome (44). Reads were then deduplicated and GC biases were corrected using the deepTools software package (45). Sequencing quality was validated using Picard to assess mapping efficiency, GC bias, and duplication rate, as well as MethylDackel for WGBS libraries to measure bisulfite conversion efficiency.

Tumor fraction ratio (TFR) was measured to assess changes in ctDNA using CNAs and local changes in cfDNA fragment length, both assessed from sequencing data. CNAs were detected using a pipeline based on ichorCNA (22) and custom algorithms. Normalized fragment length was computed by normalizing by library and genomic location. Background

signals for CNA and fragment length were established for each sequencing protocol using healthy normal samples taken from 44 individuals with no current or prior diagnosis of any malignancy (Supplementary Table S2). To maximize sensitivity of CNAs while preventing false-positive detections, Spearman rank correlation between local mean fragment length and copy number was used as a disqualifier of CNA call sets (21, 46).

To assess changes in ctDNA over time, direct comparison of the CNA-derived estimate of absolute tumor fraction between time points was not always reliable due to ambiguity, in which read depth levels correspond to each structural event. To circumvent this, CNAs were compared longitudinally with a linear model to quantify TFR. To determine confident calls, measured changes were compared with a simulated background model. No longitudinal comparisons of samples from 44 healthy participants (Supplementary Table S2) showed a significant change in TFR (e.g., Supplementary Fig. S1). Cases that showed a confident increase in tumor fraction indicated by TFR greater than 1 at either timepoint were retrospectively classified as molecular progression (MP). Major molecular response (MMR) was defined as a TFR < 0.1, an arbitrary cutoff (1 log reduction) selected prior to PFS and OS assessment.

### Statistical analysis

For the purposes of calculating sensitivity and specificity, assay results of MP were compared with a current standard of clinical or radiographic PD at FFUI. Confidence intervals (CI) on these metrics were computed with the Wilson score interval method. Survival curves were generated using the Kaplan–Meier method for PFS and OS. The Cox proportional hazards model was used to analyze the association of assay results and clinical covariates to PFS and OS. The proportional hazards assumption was evaluated with a score test on Schoenfeld residuals (47). Differences in survival were assessed with the Wald test. For two groups in the subset analysis, the Cox regression did not converge due to the small number of events in these subgroups (immunotherapy PFS and endocrine/targeted therapy OS), so a ridge penalty was applied to assay results (48). For multivariate analysis, line of therapy was grouped into treatment naïve (first-line of therapy) and previously treated (second or greater line). All *P* values were two-sided. Statistical analyses of survival were performed with the R survival package version 2.41–3 and other statistical analyses were determined using the python scipy package version 1.1.0.

## Results

### Patient characteristics

A total of 96 patients with advanced cancer, who met the inclusion criteria of the study were sequenced for the analysis (Supplementary Fig. S2). Baseline blood samples failed sequencing for five participants and were therefore excluded. The remaining 91 patients with NGS and clinical outcome data were included in this analysis. The median age was 70 years and 55% were females (Table 1). Sixty three percent of patients were current or former smokers (Supplementary Table S3). About half of the participants received a first-line therapy (53%) and 25% received a second-line therapy. The majority of patients had lung cancer (44%) or breast cancer (26%), with the remainder of the cohort representing other

cancer types (30%) including gastrointestinal cancers, genitourinary cancers, melanoma, and sarcoma (see Table 1). During the study, 46% of all participants received chemotherapy (± antibody treatment, i.e., trastuzumab, pertuzumab, panitumumab, ramucirumab, bevacizumab, and olaratumab) and 37% received immunotherapy with or without chemotherapy or a histone deacetylase inhibitor (Table 1; Supplementary Table S4).

FFUI occurred a median of 69 days after treatment start (Fig. 1B; minimum = 26 days; maximum = 208 days). Three participants received an outcome assignment based on clinical evaluation. Of these three participants, one had a nonevaluable imaging study and was assessed as clinical nonPD, and two did not have an imaging study prior to treatment change due to clinical PD assessed by the treating physician. Among the clinical variables, we found that only prior treatment was associated with PD at FFUI (OR, 0.26; $P = 0.0090$; Supplementary Table S5). The median follow-up time of the full cohort was 384 days (minimum = 60 days, maximum = 754 days).

Baseline blood samples were collected prior to treatment start for all patients (Fig. 1B; median = 0 days after treatment start, earliest 19 days before treatment start). One or two posttreatment samples were collected for each patient, with T1 collected prior to the second cycle of therapy at a median of 21 days after treatment start ($n = 85$, minimum = 14 days, maximum = 40 days) and T2 collected prior to the third cycle of therapy at a median of 42 days ($n = 66$, minimum = 37 days, maximum = 84 days). Both posttreatment samples were collected for 60 patients.

## Serial measurements of ctDNA showed early changes after treatment initiation

We assessed changes in tumor fraction using WG analysis to quantify the TFR between baseline and posttreatment samples. Substantial changes in TFR were observed early after treatment initiation (Fig. 2). In one case, we observed a rapid increase in TFR at T1 following the first cycle of therapy, indicating a major increase from baseline. This was followed by an even greater increase at T2 (Fig. 2A–D) and later an assessment of PD at FFUI. The strong pattern of CNAs was corroborated by the fragmentation pattern (Fig. 2B and C). Conversely, we observed another case with the opposite pattern with a decrease in TFR at T1 and then a larger decrease at T2 (Fig. 2E), indicating response to treatment.

A subset of samples had both WGS and WGBS and were used to test whether TFR could be quantified equivalently across sequencing protocols (Supplementary Fig. S3). TFR values were highly concordant between WGS and WGBS, enabling analysis of the full cohort including samples analyzed with both protocols.

## Changes in tumor fraction at early time points predicted radiographic progression

At FFUI, 24 of 91 patients had PD and 67 had nonPD. To evaluate the predictive value of the ctDNA assay, we compared the classification of MP with FFUI for all patients (Fig. 3A). All 13 patients with an MP at either T1 or T2 had PD, and of the 67 patients who were nonPD, none had MP. The sensitivity of the assay including time points T1 and T2 was 54% and specificity was 100%. The sensitivity was 41% at T1 and was 65% at T2 (Fig. 3B). While the sensitivity at individual time points increased between T1 and T2, there was no statistically significant relationship between sensitivity and timing of the blood draw

(Kolmogorov–Smirnov test, $P = 0.077$; Supplementary Fig. S4). In cases where MP was called, the timepoint where it was first identified preceded the detection of progression by standard-of-care imaging by a median of 39 days (Fig. 3C).

Among the 11 patients with PD at FFUI for whom MP was not called on either timepoint, three had no confident CNAs detected, two had no significant change in tumor fraction, and six had a decrease in tumor fraction. There were no major differences in predictive performance between WGS and WGBS (Supplementary Table S6).

## Molecular response assessment correlated with PFS and OS

We examined PFS and OS to evaluate the predictive value of early molecular response assessment. The full cohort of patients ($n = 91$) had median PFS of 255 days and median OS of 600 days (Supplementary Fig. S5). Patients with MP at either T1 or T2 ($n = 13$) had significantly shorter PFS [HR, 11.5 (95% CI, 5.4–24.9); $P = 4.2 \times 10^{-10}$], with a median PFS of 62 days versus 310 days for patients with no MP ($n = 78$; Fig. 3D). These patients also had significantly shorter OS [HR, 5.0 (95% CI, 2.3–10.6); $P = 3.6 \times 10^{-5}$], with 255 days median OS for patients with MP ($n = 13$) and OS median not reached for those with no MP ($n = 78$; Fig. 3E).

Clinical covariates may also contribute to survival in our heterogeneous cohort. In univariate analysis (Supplementary Table S7) prior treatment was the only clinical variable associated with PFS ($P = 0.0038$), and none of the clinical covariates were significantly associated with OS. In multivariate analysis, we found that after controlling for line of therapy (Supplementary Table S8), MP remained strongly associated with both PFS and OS.

We explored the predictive performance in subgroups based on tumor origin (Fig. 3F; Supplementary Fig. S6) and treatment type (Fig. 3G; Supplementary Fig. S7). Subgroups included lung cancer ($n = 40$), breast cancer ($n = 24$), and other cancers ($n = 27$). We found that MP was significantly associated with both PFS and OS in both lung cancer and breast cancer subsets, and with PFS but not OS in the remaining cases. Subgroups based on the type of systemic therapy received included immunotherapy (with or without chemotherapy or histone deacetylase inhibitor, $n = 34$), chemotherapy (with or without targeted or endocrine therapy, $n = 42$), and other patients ($n = 15$) who were on targeted and/or endocrine therapy alone. While MP was significantly associated with OS for the immunotherapy and chemotherapy subgroups, the association did not reach significance for the smaller subgroup of endocrine and/or targeted therapy. However, MP was significantly associated with PFS for all treatment type subgroups. In addition, we found that MP was significantly associated with both PFS and OS for subsets of patients who were treatment naïve or had prior lines of treatment (Supplementary Fig. S8). Predictions of radiographic progression also had comparable performance across these subsets (Supplementary Table S9).

Next, we analyzed MP in the context of patients with PD at FFUI (Supplementary Fig. S9) to determine whether the assay provided additional predictive value. We found that among these cases, those with MP tended to have shorter OS, however, the difference was not significant [HR, 1.7 (95% CI, 0.64–4.69)].

### MMR early on treatment predicted long-term outcome

We hypothesized that a large quantitative reduction early in the treatment course would be associated with an improved outcome. Of the 78 patients with no MP, 27 had an MMR at either posttreatment timepoint, defined as a 10-fold decrease in TFR. Notably, in all cases where an MMR was identified at T1, this finding was also observed at T2, if that timepoint was available ($n = 12$). In seven cases the TFR from baseline did not reach a 10-fold reduction at T1 but did at T2 (as in Fig. 2E).

We found that patients with an MMR ($n = 27$) had longer PFS [Fig. 4A; MMR: median PFS of 749 days, HR = 0.45 (95% CI 0.22–0.92), $P = 0.028$; Supplementary Table S10) compared with patients with no MP and no MMR ($n = 51$; median PFS of 211 days). These patients also had significantly longer OS [Fig. 4B; MMR: OS median not reached, HR = 0.116 (95% CI, 0.027–0.496), $P = 0.0036$] compared with patients with no MP and no MMR (median OS of 546 days). A multivariate analysis controlling for line of therapy (Supplementary Table S11) showed that MMR remained significantly associated with OS, although the association was not significant for PFS.

Next, we sought to assess the predictive value of an MMR in the context of radiographic response monitoring. For patients with radiographic PR or SD at FFUI ($n = 66$), the radiographic assessment of PR or SD had limited prognostic value for PFS [Fig. 4C; HR, 0.62 (95% CI, 0.30–1.25)] or OS [Fig. 4D; HR, 0.50 (95% CI, 0.19–1.36)]. Among the same subset, patients with an MMR ($n = 25$) had substantially longer PFS [HR, 0.46 (95% CI, 0.20–1.02)] and OS [HR, 0.160 (95% CI, 0.037–0.699)] than patients with no MP and no MMR ($n = 41$; Fig. 4E and F; Supplementary Fig. S10). These results indicate that early quantitative ctDNA dynamics have value for predicting long-term treatment efficacy, beyond what is known from initial radiographic assessment.

### Longitudinal changes in methylation levels may complement tumor fraction changes

For the subset of cases evaluated with WGBS ($n = 38$), methylation could additionally be used to identify changes in ctDNA. To assess the potential of this approach, we retrospectively examined two cases. A marked increase in methylation was observed for one case with nonPD at FFUI (Fig 5A), indicating a reduction over time of cancer-associated signal, despite no detectable CNAs. Another case with PD at FFUI showed a general decrease in methylation, which was consistent with a clear MP (TFR = 2.01). These cases suggest that methylation may add complementary information to CNAs and fragmentation patterns.

## Discussion

Patients with advanced malignancies require careful treatment monitoring to assess therapeutic efficacy, promote quality of life, and limit drug toxicity. Current methods for disease monitoring using clinical and radiographic assessment often require several months to confidently determine treatment response. Learning this result with high predictive value at an earlier timepoint would be a major improvement in the management of advanced cancers by significantly accelerating the feedback loop regarding therapy effectiveness.

Here, we assessed the utility of a novel, WG cfDNA molecular response assay, which analyzed longitudinal ctDNA measurements at baseline and during the initial cycles of treatment to identify response to therapy. This technique identified disease progression with a specificity of 100% and was also significantly associated with long-term survival. Moreover, MP calls were performed at a median of 6 weeks before clinical or radiographic methods confirmed these assessments. A number of prior studies have evaluated longitudinal ctDNA dynamics to assess tumor response to systemic therapy. Several of these studies have found strong concordance with survival endpoints (12, 35, 37, 38). In addition, ctDNA biomarkers have been shown to be associated with outcome assessed by imaging (37, 38), including for patients on immunotherapy (49) or tyrosine kinase inhibitors (40). Together, these and our findings indicate that ctDNA changes in the blood reflect treatment response and resistance early in the course of treatment, likely before changes in the shape, density, or size of the target lesions on imaging.

Furthermore, we demonstrated that patients with an MMR had a longer PFS and OS compared with those with no change or a smaller decrease in TFR, indicating that there was quantitative value in the degree of initial response to therapy. The additional prognostic value of identifying an MMR supports the potential to integrate imaging and analysis of serial cfDNA samples to provide an early indication of an extended duration of disease control.

We also performed subset analyses of the two cohorts with the largest number of patients by cancer type (lung and breast cancer) and by treatment modality (chemotherapy and immunotherapy), which demonstrated a strong association between MP and PFS and OS. For the “other” subgroup of patients based on cancer site and treatment type, MP was only associated with PFS but not OS. These groups were more heterogeneous and had smaller sample sizes compared with breast and lung cancers and chemotherapy and immunotherapy groups. However, the larger subgroup analyses suggested that the WG ctDNA assay might have potential in different clinical scenarios by looking beyond targeted assessment of tumor-specific point mutations and amplifications.

While many prior studies have focused on point mutations, a challenge for these methods is that they must reliably select driver or truncal mutations in each individual case, a process that may need to be calibrated for cancer and treatment type. A common approach is based on tumor tissue sequencing to identify mutations for tracking, but access to adequate tissue varies by tumor type and may be limiting in an advanced disease setting. In many situations, biopsies are difficult to perform and run the risk of missing relevant clonal mutations, given the genetic heterogeneity of metastatic lesions. In contrast, low-coverage WG approaches can be used to detect (21, 22) and track changes (49) at low cost based on blood samples alone.

This study has several limitations. First, despite this being a prospectively enrolled study, there were a number of protocol deviations reflecting a wide range of clinical practice patterns. About 30% of participants in the ongoing study were not properly enrolled or followed, hence, were excluded from this analysis. Other minor deviations were variations in sample collection and imaging time points, which did not warrant exclusion from the

analysis. Otherwise, we made every effort to include participants who met the inclusion criteria and had blood collections from at least two time points to avoid introducing bias. The excluded participants were missing baseline imaging assessment, having baseline sample collected after treatment initiation, or T1 sample collection date exceeded FFUI date. One study site was responsible for the large proportion of this oversight (80%). Inclusion of these participants resulted in heavy representation of one study site in the study population, which may limit the generalizability of the results.

Second, while the specificity of the assay was very high, which is the critical performance metric for clinical utility in the advanced setting, sensitivity to identify clinical progression early in the treatment course was relatively low. Sensitivity, particularly at the earliest timepoint, may be improved by including other features such as cancer-associated epigenetic signals. In future work, we plan to incorporate these methylation-based signals into the assay, along with fragment length and copy-number information with the goal of increasing assay sensitivity. However, even with additional orthogonal signals, there will still be a residual false-negative rate from (i) tumors that do not generate sufficient ctDNA (i.e., nonshedding tumors), (ii) tumors that have not yet progressed during the earliest cycles of treatment, and (iii) tumors in which MP by ctDNA analysis and imaging are not in agreement.

Third, the study was not sufficiently powered to draw conclusions from the subgroup analyses, particularly in treatments that were less represented (e.g., targeted or endocrine therapy) and tumors with fewer patients, particularly nonlung and nonbreast cancers. Currently, we cannot draw adequate conclusions about the predictive nature of the assay in these small cohorts of patients. However, because there was a significant main effect, we explored the assay’s predictive ability across different cancer and treatment types. We hypothesized that the dynamics of early changes in cancer-associated signals in the blood identified by WGS are agnostic to cancer type as the initial results of this study suggest. Prospective validation studies using more homogenous patient cohorts with appropriate sample sizes are needed to validate this assay in each of these clinical settings.

If further validated in an adequately powered prospective clinical validation study, molecular response monitoring with serial measurements of cfDNA has potential clinical benefits for both assessing disease progression and disease control. An early call of MP could lead oncologists to consider discontinuation of ineffective treatments, thereby reducing avoidable side effects and financial toxicity. By accelerating the clinical feedback loop, patients would be afforded the opportunity to change to an alternative, potentially effective therapy. In contrast, MMR could provide confidence in the current treatment plan, and encourage clinicians and patients to maintain the course and potentially reduce the frequency of imaging. In addition, new adaptive approaches should be considered with MMR as the interim endpoint in clinical trials. Moreover, a blood-based assay provides convenience for patients as blood samples are collected routinely during the course of therapy. Patients may have improved outcomes by limiting side effects and costs associated with ineffective treatments, trying alternate potentially effective treatments earlier, and feeling encouraged with early exceptional response to maintain the course.

In conclusion, we demonstrated that identifying disease progression through earlier low-pass WG ctDNA–based monitoring was concordant with standard-of-care clinical assessment, and the degree of ctDNA reduction was strongly correlated with long-term outcome. These findings appeared consistent across several tumor and treatment types. The assay captured changes in tumor biology that occurred early in the course of systemic therapy, which were observed before confident radiographic detection of these changes was possible. If validated prospectively, this noninvasive tool would allow oncologists and patients to understand response and resistance to treatment in a more precise and timely way.

## Supplementary Material

Refer to Web version on PubMed Central for supplementary material.

## Acknowledgments

This study was supported by Lexent Bio, Inc. We thank all participants and their families for participating in this study. We also thank Dr. Brian McNamee for review of all clinical images, as well as all clinicians and their research staff.

The costs of publication of this article were defrayed in part by the payment of page charges. This article must therefore be hereby marked *advertisement* in accordance with 18 U.S.C. Section 1734 solely to indicate this fact.

Disclosure of Potential Conflicts of Interest

A.A. Davis has received travel support from Menarini Silicon Biosystems. W.T. Iams is a consultant (paid consultant) at Genentech, Outcomes Insights, and Defined Health, and has provided expert testimony for O'Neil, Parker, & Williamson, PLLC and Susan Blasik-Miller, Freud, Freeze, & Arnold. N. Peterman is a senior computational biologist (paid consultant) at and has ownership interest (including patents) in Lexent Bio. A. Robertson is a director of computational biology (paid consultant) at Lexent Bio, is a bioinformatics engineer at Color Genomics, and has ownership interest (including patents) in Counsyl. A. Shah is a VP engineer (paid consultant) at Lexent Bio and has ownership interest (including patents) in Myriad Genetics. R. Srivas is a computational biologist (paid consultant) at and has ownership interest (including patents) in Lexent Bio. N.J. Lambert is a director (paid consultant) at Lexent Bio. H.W. Wood is a research associate (paid consultant) at and has ownership interest (including patents) in Lexent Bio. J.C. Close has ownership interest (including patents) in Lexent Bio. A. Tezcan is head of clinical development (paid consultant) at Lexent Bio Inc. K. Nesmith is CEO (paid consultant) at Lexent Bio, is a senior director at Counsyl, and has ownership interest (including patents) in Lexent Bio. H. Tezcan is CMO (paid consultant) at Lexent Bio. Y.K. Chae reports receiving commercial research grant from AbbVie, BMS, Biodesix, Freenome, and Lexent Bio and reports receiving speakers bureau honoraria from BMS, AstraZeneca, Genentech, Foundation Medicine, Guardant Health, Lilly Oncology, Takeda, and Pfizer. No potential conflicts of interest were disclosed by the other authors.

## References

1. Eisenhauer EA, Therasse P, Bogaerts J, Schwartz LH, Sargent D, Ford R, et al. New response evaluation criteria in solid tumours: revised RECIST guideline (version 1.1). Eur J Cancer 2009;45:228–47. [PubMed: 19097774]
2. Seymour L, Bogaerts J, Perrone A, Ford R, Schwartz LH, Mandrekar S, et al. iRECIST: guidelines for response criteria for use in trials testing immunotherapeutics. Lancet Oncol 2017;18:e143–52. [PubMed: 28271869]
3. Erasmus JJ, Gladish GW, Broemeling L, Sabloff BS, Truong MT, Herbst RS, et al. Interobserver and intraobserver variability in measurement of non-small-cell carcinoma lung lesions: implications for assessment of tumor response. J Clin Oncol 2003;21:2574–82. [PubMed: 12829678]
4. Nishino M, Giobbie-Hurder A, Manos MP, Bailey N, Buchbinder EI, Ott PA, et al. Immune-related tumor response dynamics in melanoma patients treated with pembrolizumab: identifying markers for clinical outcome and treatment decisions. Clin Cancer Res 2017;23:4671–9. [PubMed: 28592629]

5. Chiou VL, Burotto M. Pseudoprogression and immune-related response in solid tumors. J Clin Oncol 2015;33:3541–3. [PubMed: 26261262]
6. Kuhl CK, Alparslan Y, Schmoee J, Sequeira B, Keulers A, Brümmendorf TH, et al. Validity of RECIST version 1.1 for response assessment in metastatic cancer: a prospective, multireader study. Radiology 2019;290:349–56. [PubMed: 30398433]
7. Wan JCM, Massie C, Garcia-Corbacho J, Mouliere F, Brenton JD, Caldas C, et al. Liquid biopsies come of age: towards implementation of circulating tumour DNA. Nat Rev Cancer 2017;17:223–38. [PubMed: 28233803]
8. Siravegna G, Marsoni S, Siena S, Bardelli A. Integrating liquid biopsies into the management of cancer. Nat Rev Clin Oncol 2017;14:531–48. [PubMed: 28252003]
9. Heitzer E, Ulz P, Geigl JB. Circulating tumor DNA as a liquid biopsy for cancer. Clin Chem 2015;61:112–23. [PubMed: 25388429]
10. Chen K-Z, Lou F, Yang F, Zhang J-B, Ye H, Chen W, et al. Circulating tumor DNA detection in early-stage non-small cell lung cancer patients by targeted sequencing. Sci Rep 2016;6:31985. [PubMed: 27555497]
11. Merker JD, Oxnard GR, Compton C, Diehn M, Hurley P, Lazar AJ, et al. Circulating tumor DNA analysis in patients with cancer: American Society of Clinical Oncology and College of American Pathologists joint review. J Clin Oncol 2018;36:1631–41. [PubMed: 29504847]
12. Murtaza M, Dawson S-J, Tsui DWY, Gale D, Forshew T, Piskorz AM, et al. Noninvasive analysis of acquired resistance to cancer therapy by sequencing of plasma DNA. Nature 2013;497:108–12. [PubMed: 23563269]
13. Chan KCA, Jiang P, Zheng YWL, Liao GJW, Sun H, Wong J, et al. Cancer genome scanning in plasma: detection of tumor-associated copy number aberrations, single-nucleotide variants, and tumoral heterogeneity by massively parallel sequencing. Clin Chem 2013;59:211–24. [PubMed: 23065472]
14. Mouliere F, Robert B, Arnau Peyrotte E, Del Rio M, Ychou M, Molina F, et al. High fragmentation characterizes tumour-derived circulating DNA. PLoS One 2011;6:e23418. [PubMed: 21909401]
15. Jiang P, Chan CWM, Chan KCA, Cheng SH, Wong J, Wong VW-S, et al. Lengthening and shortening of plasma DNA in hepatocellular carcinoma patients. Proc Natl Acad Sci U S A 2015;112:E1317–25. [PubMed: 25646427]
16. Underhill HR, Kitzman JO, Hellwig S, Welker NC, Daza R, Baker DN, et al. Fragment length of circulating tumor DNA. PLoS Genet 2016;12: e1006162. [PubMed: 27428049]
17. Snyder MW, Kircher M, Hill AJ, Daza RM, Shendure J. Cell-free DNA comprises an in vivo nucleosome footprint that informs its tissues-of-origin. Cell 2016;164: 57–68. [PubMed: 26771485]
18. Jiang P, Sun K, Tong YK, Cheng SH, Cheng THT, Heung MMS, et al. Preferred end coordinates and somatic variants as signatures of circulating tumor DNA associated with hepatocellular carcinoma. Proc Natl Acad Sci U S A 2018;115: E10925–33. [PubMed: 30373822]
19. Sun K, Jiang P, Chan KCA, Wong J, Cheng YKY, Liang RHS, et al. Plasma DNA tissue mapping by genome-wide methylation sequencing for noninvasive prenatal, cancer, and transplantation assessments. Proc Natl Acad Sci U S A 2015; 112:E5503–12. [PubMed: 26392541]
20. Beroukhim R, Mermel CH, Porter D, Wei G, Raychaudhuri S, Donovan J, et al. The landscape of somatic copy-number alteration across human cancers. Nature 2010;463:899–905. [PubMed: 20164920]
21. Mouliere F, Chandrananda D, Piskorz AM, Moore EK, Morris J, Ahlborn LB, et al. Enhanced detection of circulating tumor DNA by fragment size analysis. Sci Transl Med 2018;10:eaat4921. [PubMed: 30404863]
22. Adalsteinsson VA, Ha G, Freeman SS, Choudhury AD, Stover DG, Parsons HA, et al. Scalable whole-exome sequencing of cell-free DNA reveals high concordance with metastatic tumors. Nat Commun 2017;8:1324. [PubMed: 29109393]
23. Hon GC, Hawkins RD, Caballero OL, Lo C, Lister R, Pelizzola M, et al. Global DNA hypomethylation coupled to repressive chromatin domain formation and gene silencing in breast cancer. Genome Res 2012;22:246–58. [PubMed: 22156296]

24. Chan KCA, Jiang P, Chan CWM, Sun K, Wong J, Hui EP, et al. Noninvasive detection of cancer-associated genome-wide hypomethylation and copy number aberrations by plasma DNA bisulfite sequencing. Proc Natl Acad Sci U S A 2013; 110:18761–8. [PubMed: 24191000]
25. Usadel H, Brabender J, Danenberg KD, Jerónimo C, Harden S, Engles J, et al. Quantitative adenomatous polyposis coli promoter methylation analysis in tumor tissue, serum, and plasma DNA of patients with lung cancer. Cancer Res 2002;62:371–5. [PubMed: 11809682]
26. Pantel K, Alix-Panabières C. Liquid biopsy and minimal residual disease - latest advances and implications for cure. Nat Rev Clin Oncol 2019;16:409–24. [PubMed: 30796368]
27. Abbosh C, Birkbak NJ, Swanton C. Early stage NSCLC - challenges to implementing ctDNA-based screening and MRD detection. Nat Rev Clin Oncol 2018; 15:577–86. [PubMed: 29968853]
28. Chae YK, Oh MS. Detection of minimal residual disease using ctDNA in lung cancer: current evidence and future directions. J Thorac Oncol 2019;14: 16–24. [PubMed: 30296486]
29. Rossi G, Ignatiadis M. Promises and pitfalls of using liquid biopsy for precision medicine. Cancer Res 2019;79:2798–804. [PubMed: 31109952]
30. Lanman RB, Mortimer SA, Zill OA, Sebisanovic D, Lopez R, Blau S, et al. Analytical and clinical validation of a digital sequencing panel for quantitative, highly accurate evaluation of cell-free circulating tumor DNA. PLoS One 2015; 10:e0140712. [PubMed: 26474073]
31. Diaz LA, Bardelli A. Liquid biopsies: genotyping circulating tumor DNA. J Clin Oncol 2014;32:579–86. [PubMed: 24449238]
32. Reckamp KL, Melnikova VO, Karlovich C, Sequist LV, Camidge DR, Wakelee H, et al. A highly sensitive and quantitative test platform for detection of NSCLC EGFR mutations in urine and plasma. J Thorac Oncol 2016;11:1690–700. [PubMed: 27468937]
33. Juric D, Ciruelos E, Rubovszky G, Campone M, Loibl S, Rugo HS, et al. Alpelisib + fulvestrant for advanced breast cancer: subgroup analyses from the phase III SOLAR-1 trial. [abstract]. In: Proceedings of the 2018 San Antonio Breast Cancer Symposium; 2018 Dec 4–8; San Antonio, TX. Philadelphia (PA): AACR; 2019. Abstract nr GS3–08.
34. Fribbens C, O'Leary B, Kilburn L, Hrebien S, Garcia-Murillas I, Beaney M, et al. Plasma ESR1 mutations and the treatment of estrogen receptor-positive advanced breast cancer. J Clin Oncol 2016;34:2961–8. [PubMed: 27269946]
35. Diehl F, Schmidt K, Choti MA, Romans K, Goodman S, Li M, et al. Circulating mutant DNA to assess tumor dynamics. Nat Med 2008;14:985–90. [PubMed: 18670422]
36. Dawson S-J, Tsui DWY, Murtaza M, Biggs H, Rueda OM, Chin S-F, et al. Analysis of circulating tumor DNA to monitor metastatic breast cancer. N Engl J Med 2013;368:1199–209. [PubMed: 23484797]
37. Tie J, Kinde I, Wang Y, Wong HL, Roebert J, Christie M, et al. Circulating tumor DNA as an early marker of therapeutic response in patients with metastatic colorectal cancer. Ann Oncol 2015;26:1715–22. [PubMed: 25851626]
38. Pécuchet N, Zonta E, Didelot A, Combe P, Thibault C, Gibault L, et al. Base-position error rate analysis of next-generation sequencing applied to circulating tumor DNA in non-small cell lung cancer: a prospective study. PLoS Med 2016; 13:e1002199. [PubMed: 28027313]
39. Hrebien S, Citi V, Garcia-Murillas I, Cutts R, Fenwick K, Kozarewa I, et al. Early ctDNA dynamics as a surrogate for progression free survival in advanced breast cancer in the BEECH trial. Ann Oncol 2019;30:945–952. [PubMed: 30860573]
40. Phallen J, Leal A, Woodward BD, Forde PM, Naidoo J, Marrone KA, et al. Early noninvasive detection of response to targeted therapy in non-small cell lung cancer. Cancer Res 2019;79:1204–13. [PubMed: 30573519]
41. Li H, Durbin R. Fast and accurate short read alignment with burrows-wheeler transform. Bioinformatics 2009;25:1754–60. [PubMed: 19451168]
42. Tarasov A, Vilella AJ, Cuppen E, Nijman IJ, Prins P. Sambamba: fast processing of NGS alignment formats. Bioinformatics 2015;31:2032–4. [PubMed: 25697820]
43. Li H, Handsaker B, Wysoker A, Fennell T, Ruan J, Homer N, et al. The sequence alignment/map format and SAMtools. Bioinformatics 2009;25: 2078–9. [PubMed: 19505943]
44. Krueger F, Andrews SR. Bismark: a flexible aligner and methylation caller for bisulfite-Seq applications. Bioinformatics 2011;27:1571–2. [PubMed: 21493656]

45. Ramírez F, Dündar F, Diehl S, Grüning BA, Manke T. deepTools: a flexible platform for exploring deep-sequencing data. Nucleic Acids Res 2014;42: W187–91. [PubMed: 24799436]

46. Hellwig S, Nix DA, Gligorich KM, O'Shea JM, Thomas A, Fuertes CL, et al. Automated size selection for short cell-free DNA fragments enriches for circulating tumor DNA and improves error correction during next generation sequencing. PLoS One 2018;13:e0197333. [PubMed: 30044795]

47. Grambsch PM, Therneau TM. Proportional hazards tests and diagnostics based on weighted residuals. Biometrika 1994;81:515–26.

48. Verweij PJ, Van Houwelingen HC. Penalized likelihood in cox regression. Stat Med 1994;13:2427–36. [PubMed: 7701144]

49. Jensen TJ, Goodman AM, Kato S, Ellison CK, Daniels GA, Kim L, et al. Genome-wide sequencing of cell-free DNA identifies copy-number alterations that can be used for monitoring response to immunotherapy in cancer patients. Mol Cancer Ther 2019;18:448–58. [PubMed: 30523049]

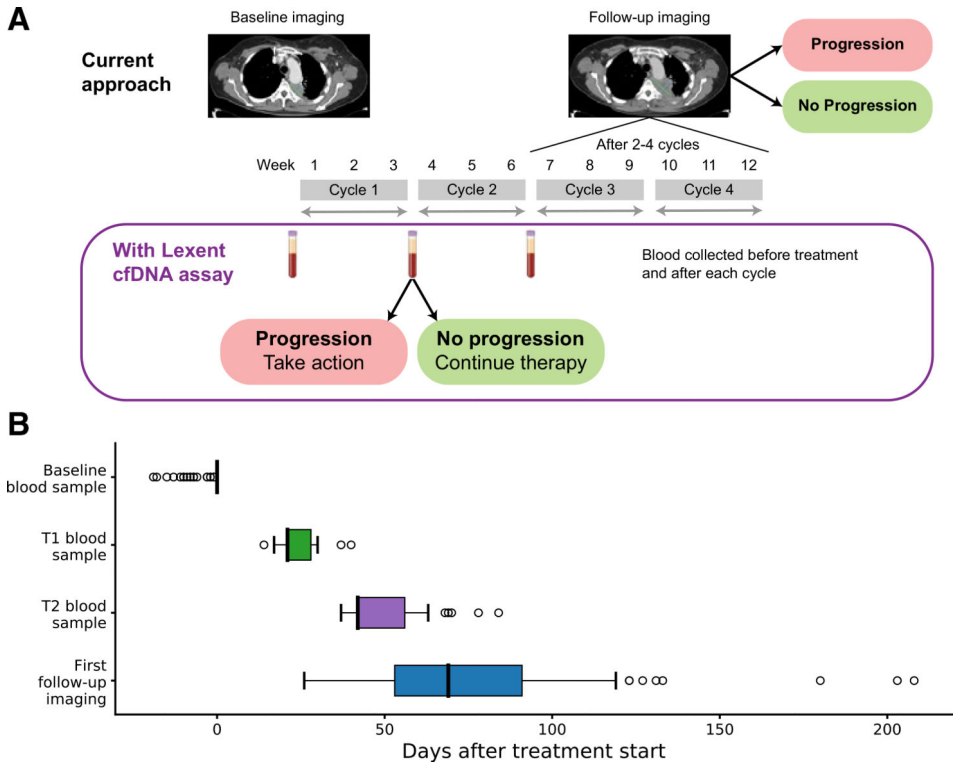


**Figure 1.**

Overview of the clinical setting. **A,** Diagram comparing radiographic response assessment and the potential use of cfDNA to assess molecular response. **B,** Timing of imaging and blood collections for patients in the study.

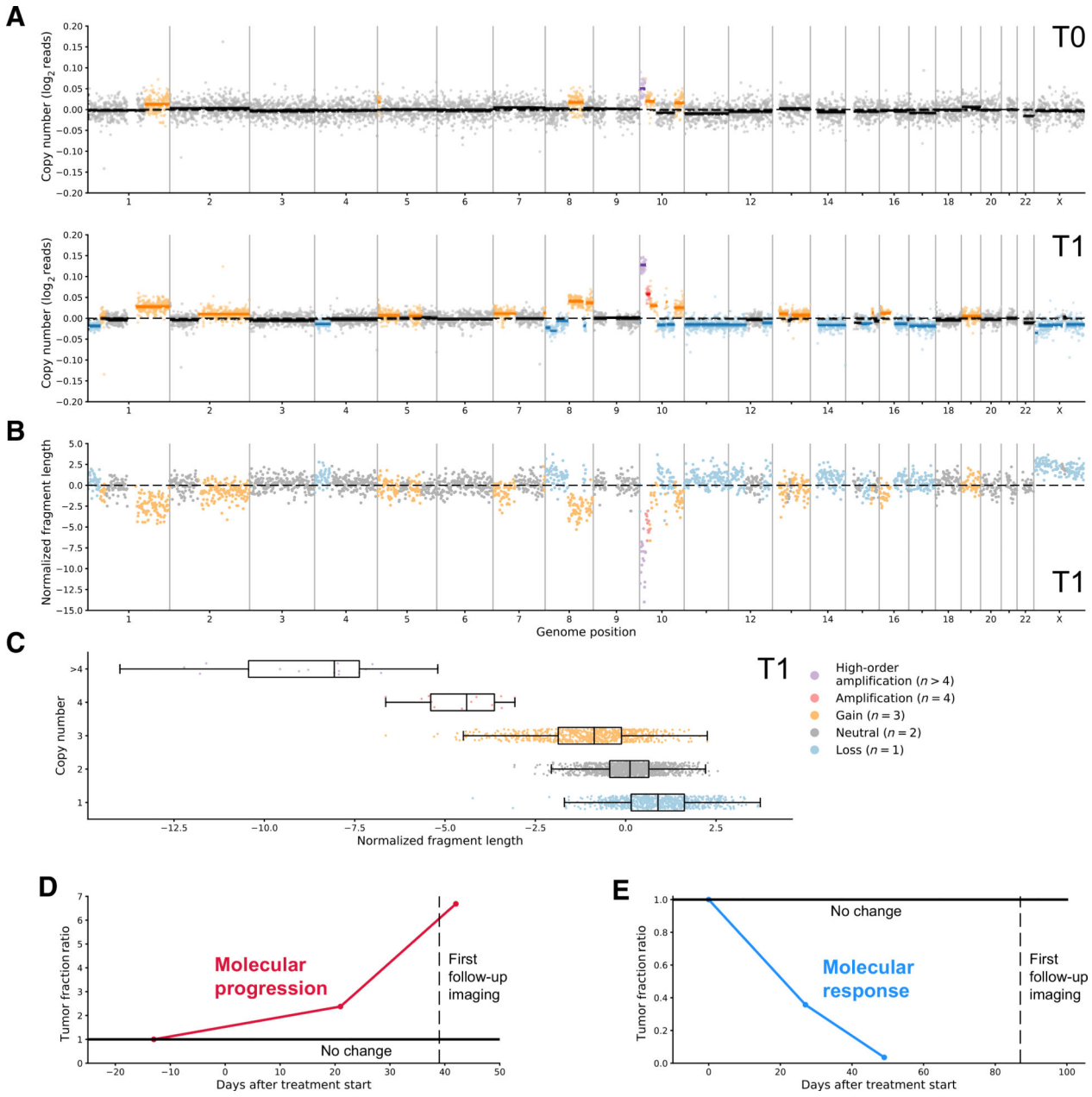


**Figure 2.**

Serial assessment of ctDNA to determine MP. **A,** The genome-wide plots of CNAs detected for 1 patient. The T0 baseline blood draw was collected 13 days before the start of treatment, and T1 was collected 21 days after the start of treatment. **B,** Normalized fragment length exhibits the reverse pattern compared with CNAs. **C,** Overall, there was a strong negative correlation between the normalized fragment length at each genomic position and the inferred copy number (Spearman rho = −0.57; $P < 10^{-10}$). **D,** This case showed an increase in TFR at follow-up time points T1 and T2, detectable in advance of imaging that indicated PD. **E,** Another case showed a marked decrease in TFR at T1 and T2, concordant with later imaging that showed PR.

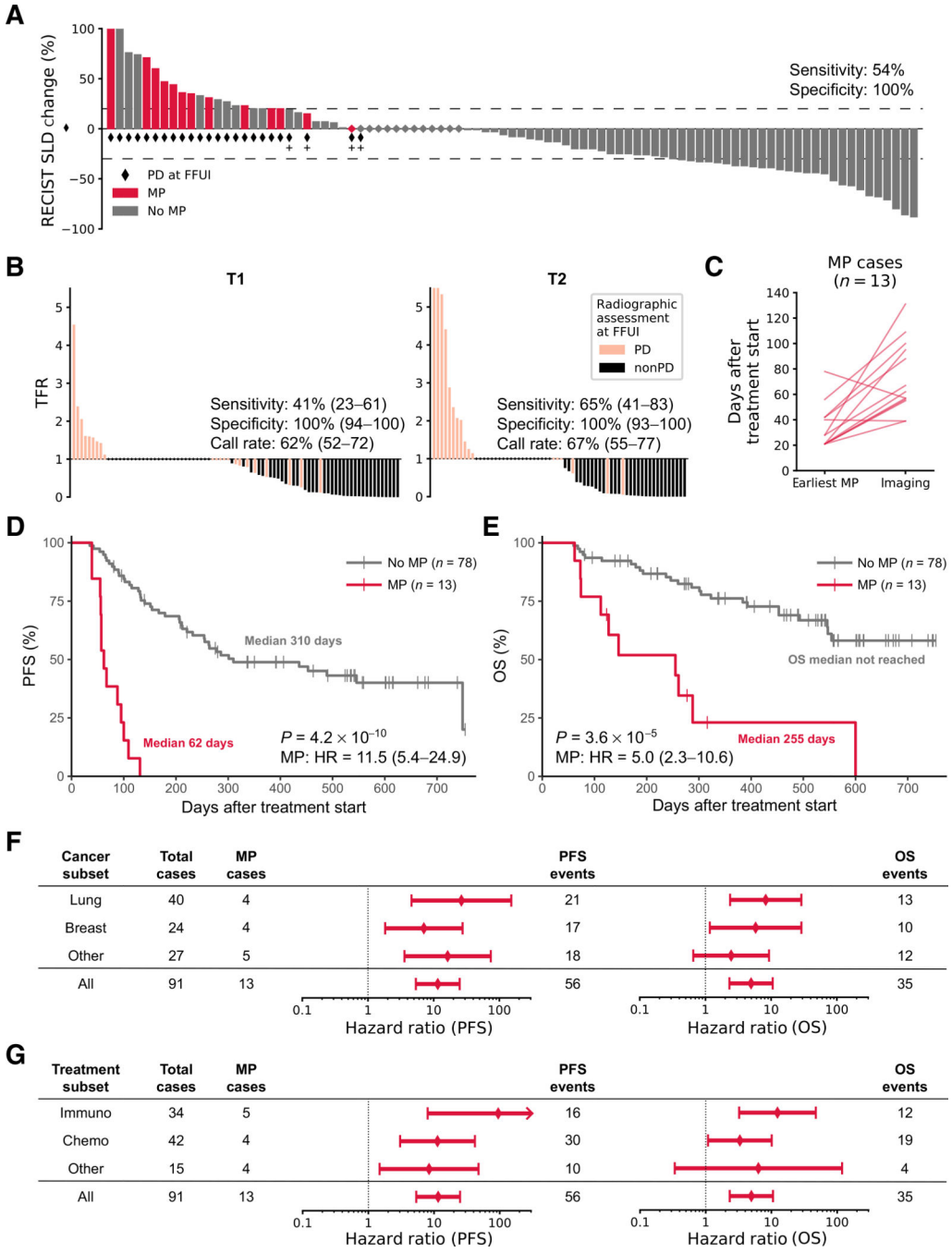


**Figure 3.**

ctDNA assessments following first or second cycle of therapy predicted progression. **A,** Comparison of imaging results at FFUI, sum of longest diameters assessed by RECIST 1.1, with ctDNA assessment of MP indicated by a confident increase in TFR for either posttreatment sample ($n = 91$, sensitivity = 54%, specificity = 100%). Cases of clinical progression are indicated by plus signs. **B,** TFR at T1 (left, $n = 85$) and T2 (right, $n = 66$) compared with radiographic or clinical assessment of PD or nonPD, showing predictive performance at each timepoint. Diamonds indicate no change. **C,** For patients with MP ($n =$

13), detection of MP was observed to precede the detection of progression by standard-of-care imaging by a median of 39 days. Two cases showed MP after FFUI, by 1 day and 21 days. PFS (**D**) and OS (**E**) for all patients grouped by MP. Patients with MP had significantly shorter PFS ($P = 4.2 \times 10^{-10}$) and OS ($P = 3.6 \times 10^{-5}$). HR with 95% CIs for cancer type subsets (**F**) and treatment modality subsets (**G**).

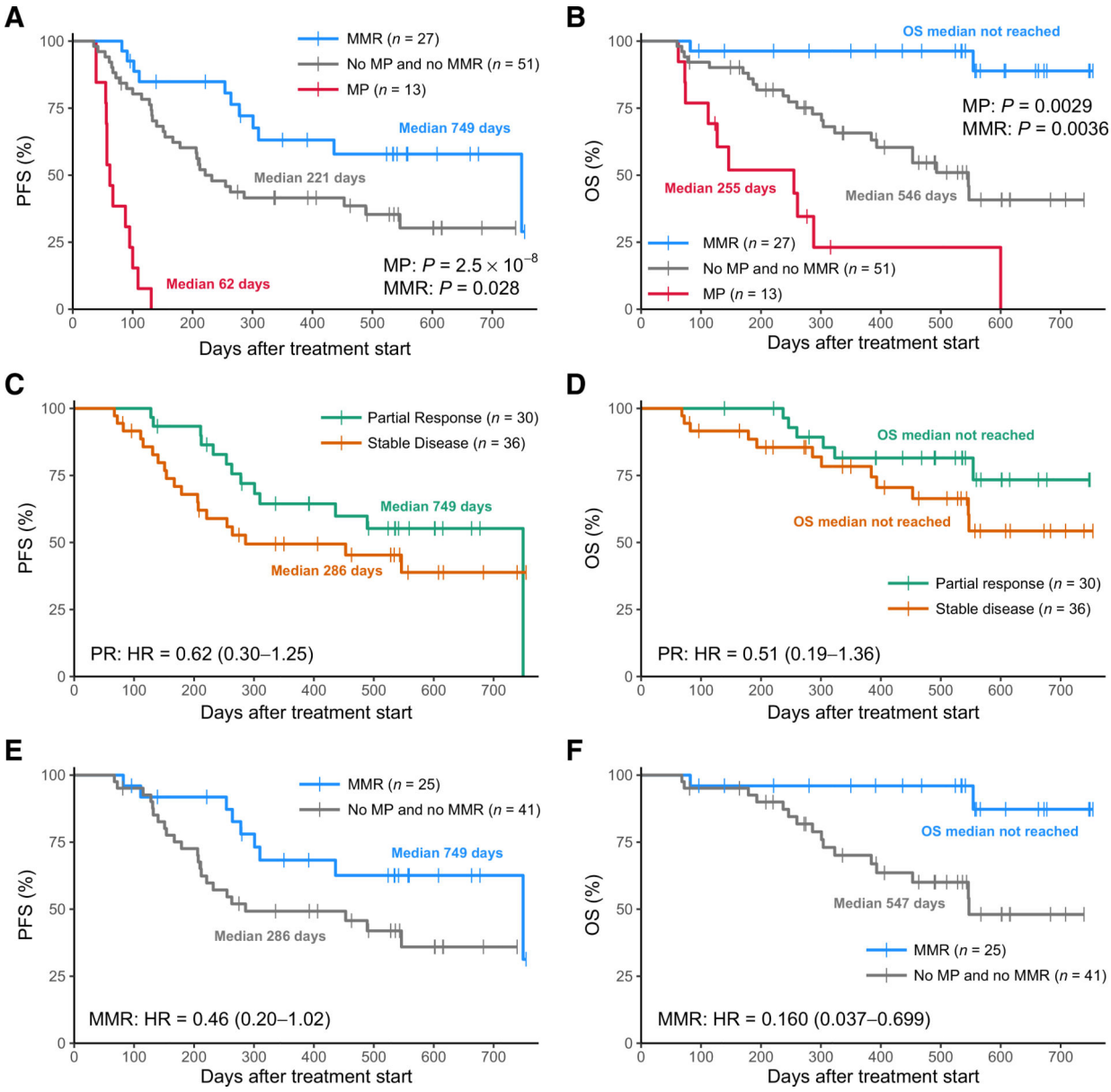


**Figure 4.**

MMR was associated with a favorable outcome. PFS (**A**) and OS (**B**) for patients with MP or MMR. Patients with MMR had significantly longer PFS ($P = 0.028$) and OS ($P = 0.0036$). Survival analysis of the subset of patients with nonPD assessed radiographically at FFUI ($N = 66$), stratified by response status at FFUI (**C** and **D**) or MMR (**E** and **F**).

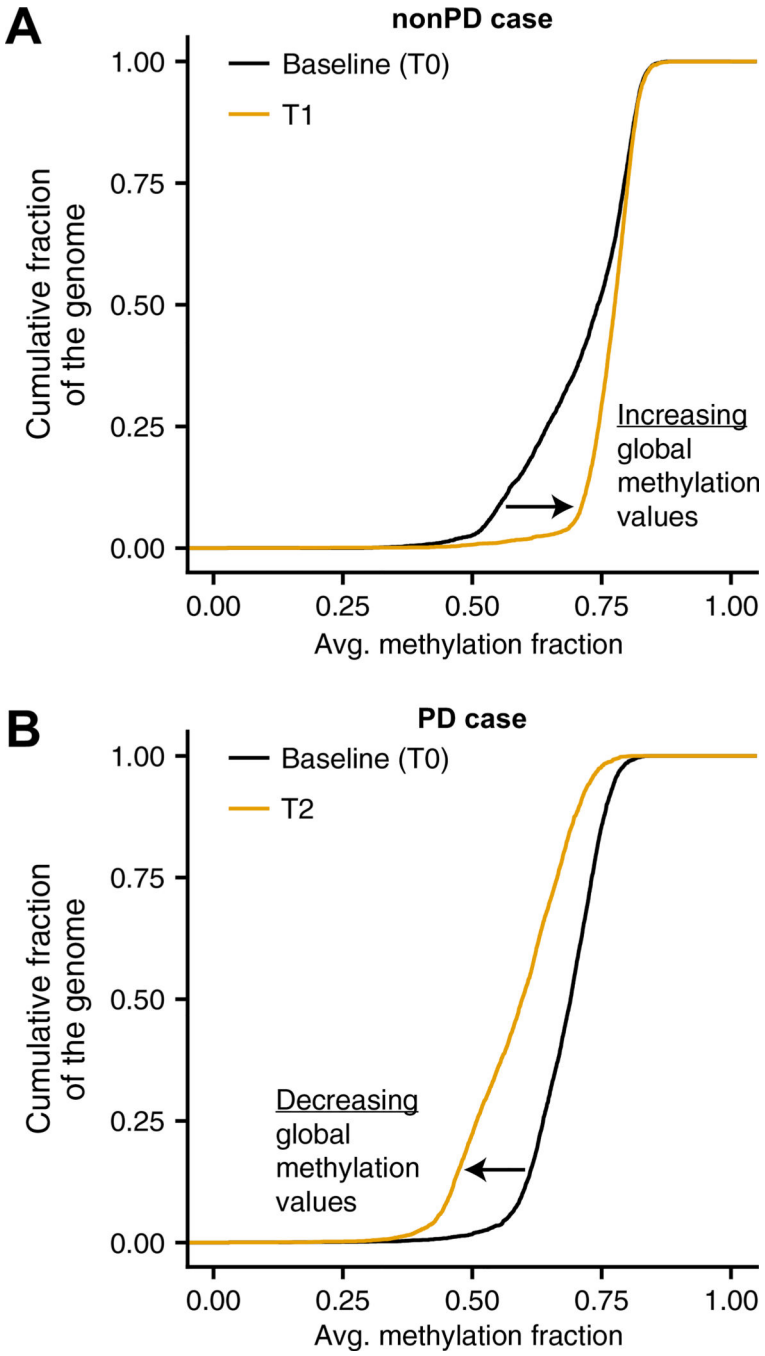


**Figure 5.**

Methylation may provide an orthogonal signal to CNAs for response monitoring. Distribution of average methylation levels in genome-wide 1 megabase bins for a patient with nonPD (**A**) and a patient with PD (**B**). Distributions are plotted at baseline and during treatment.

**Table 1.**

Patient and sample characteristics.

| | Median (min–max) | *N* = 91 (%) |
|---|---|---|
| Age | 70 (30–89) | |
| Sex | | |
| Female | | 50 (55) |
| Male | | 41 (45) |
| Cancer type | | |
| Lung | | 40 (44) |
| Breast | | 24 (26) |
| Melanoma | | 6 (7) |
| Pancreas | | 4 (4) |
| Colon | | 3 (3) |
| Rectum | | 3 (3) |
| Renal | | 3 (3) |
| Biliary | | 2 (2) |
| Stomach | | 2 (2) |
| Bladder | | 2 (2) |
| Prostate | | 1 (1) |
| Sarcoma | | 1 (1) |
| Treatment types | | |
| Chemotherapy | | 32 (35) |
| Chemotherapy, antibody | | 10 (11) |
| Immunotherapy | | 24 (26) |
| Immunotherapy, chemotherapy | | 9 (10) |
| Immunotherapy, HDACi | | 1 (1) |
| Endocrine | | 4 (4) |
| Endocrine, CDK4/6i | | 6 (7) |
| Targeted alone | | 5 (5) |
| Lines of therapy | | |
| 1 | | 48 (53) |
| 2 | | 23 (25) |
| 3+ | | 20 (22) |
| Timing (days since treatment start) | | |
| T1 | 21 (14–40) | 85 (93) |
| T2 | 42 (37–84) | 66[a] (72) |
| First follow-up | 69 (26–208) | |
| Last follow-up | 384 (60–754) | |
| Protocol | | |
| WGS | | 53 (58) |
| WGBS | | 38[b] (42) |

Abbreviation: HDACi, histone deacetylase inhibitor.

[a] Sixty had both posttreatment time points.

[b] In addition, 13 of the participants analyzed with WGS were also analyzed with WGBS.